MODELLING TRANSIENT WINDS

Mark Sterling[a], Matthew Haines[a], and Mike Jesson[a]

[a]*School of Civil Engineering, University of Birmingham, Edgbaston, Birmingham, B15 2TT, UK.*
m.sterling@bham.ac.uk

Keywords: Transient winds, thunderstorm downburst, pressure distribution

Abstract. This paper examines the flow field associated with a variety of transient winds and discussed in detail the physical and numerical simulation of a flow structure that could be interpreted as a thunderstorm downburst. The possible pressure field arising from such a structure as it impacts on a high-rise building is examined. Possible differences between such flow phenomena and those corresponding to typical boundary layer winds are observed to occur – the magnitude and importance of these differences currently remains an open point.

1 INTRODUCTION

Over the last decade, the interest in modelling the effects of transient winds and their corresponding wind loading on structures has started to grow (see for example Letchford et al., 2002; Mason et al., 2005; Lin and Savory, 2006; Durañona et al., 2009; McConville et al., 2009; Kareem, 2012; Haines et al., 2012 to name but a few). There are a variety of non-stationary, transient winds which occur around the world. However, the ones that have caught the imagination of the scientific community the most appear to be those associated with thunderstorm downbursts.

A thunderstorm can give rise to a downward movement of air (Fujita, 1985) and under the correct conditions this can impinge on the ground. The resulting air flow is then displaced radially from the point of impingement resulting in a relatively large vortex structure with horizontal axis of rotation (Figure 1). Figure 1a illustrates the presence of a large vortex structure at the edge of the downburst (in figure 1a the large vortex is visible due to dust entrainment). The generation of an idealised downburst (McConville, 2008; McConville et al., 2009) is also shown for comparison (figure 1b). In figure 1b small polystyrene balls were used to aid flow visualization and, although not neutrally buoyant, they provide a qualitative comparison.

Figure 2a illustrates the distribution of mean (time averaged) streamwise velocity with respect to height above the ground which may arise from a downburst compared to that of a typical synoptic (conventional ABL) wind; the marked difference in profiles is evident. Figure 2b illustrates that these differences are also present when examining the corresponding streamwise velocity time series at a given height above the ground. In figure 2b, AAFB denotes a downburst velocity time series that was recorded at the Andrew's Air Force Base (Fuijtia, 1985). As will be outlined in section 2, there is dearth of full-scale data and so, although the AAFB data is often assumed to represent a typical downburst, this may not necessarily be the case.

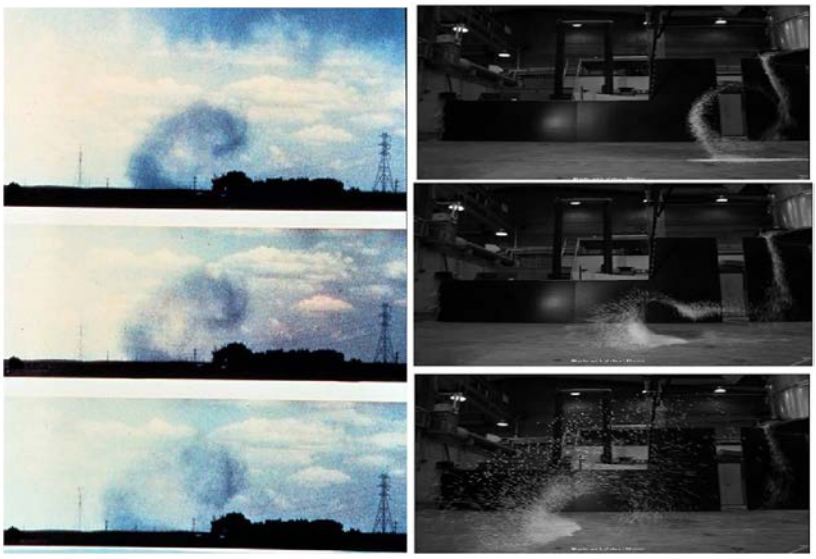

(a) NOAA photo library Image ID: nssl0106

(b) The Birmingham downburst simulator

Figure 1: A visual comparison between an actual downburst event and a physical simulation.

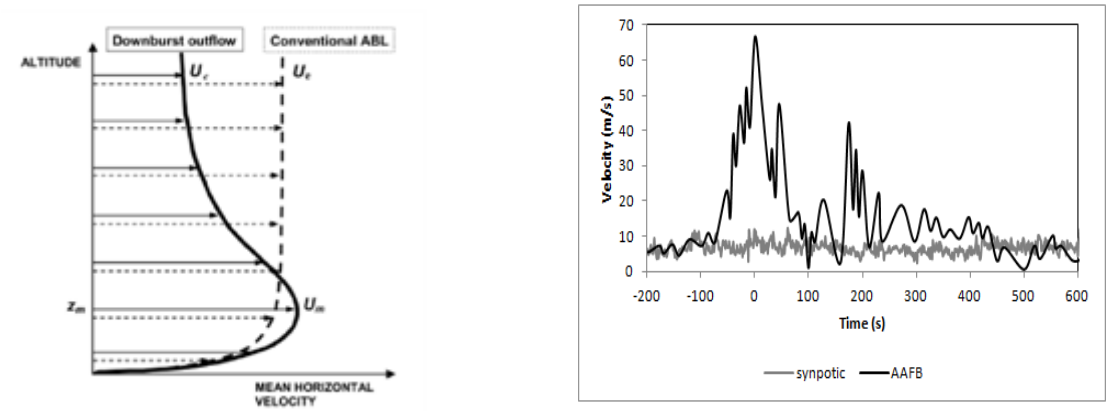

(a) Streamwise velocity profile (b) Synoptic and downburst veloicty time series

Figure 2: (a) A schematic illustration of the mean streamwise velocity profile corresponding to a 'typical' downburst and a typical boundary layer wind (Lin and Savory, 2006); (b) a comparison of a synoptic and downburst wind velocity time history.

The difference between the streamwise profiles and the time series illustrated in figure 2 arise as a result of the differences in the flow field which occurs during a downburst event compared to that of a synoptic wind (figure 1).

This paper will briefly examine the structure of some transient winds through an analysis of full-scale data (section 2), physical modeling (section 3) and numerical simulations (section 4). Closing remarks are presented in section 5.

2 FULL SCALE DATA

Perhaps the most extensive set of full-scale events recorded close to the ground can be found in Lombardo (2010), who analyzed eight recorded downbursts at the Texas Tech University field site. Figure 3 illustrates the associated velocity time series which correspond to measurements obtained ~10m above the ground. The first striking feature of figure 3 illustrates that there are large similarities between each event, i.e., a rapid change in wind velocity over a short time period can be observed. However, it can also be seen that there is a large degree of variability between events and no one event is identical. Thus, the time series shown in figure 2b corresponds to a singular event rather than representing the norm. Indeed, given the number of variables associated with each event (see section 3 and Sterling et al., 2011) there is, on reflection, no reason to assume that two recorded events would be identical even if the variation due to small-scale turbulence was removed.

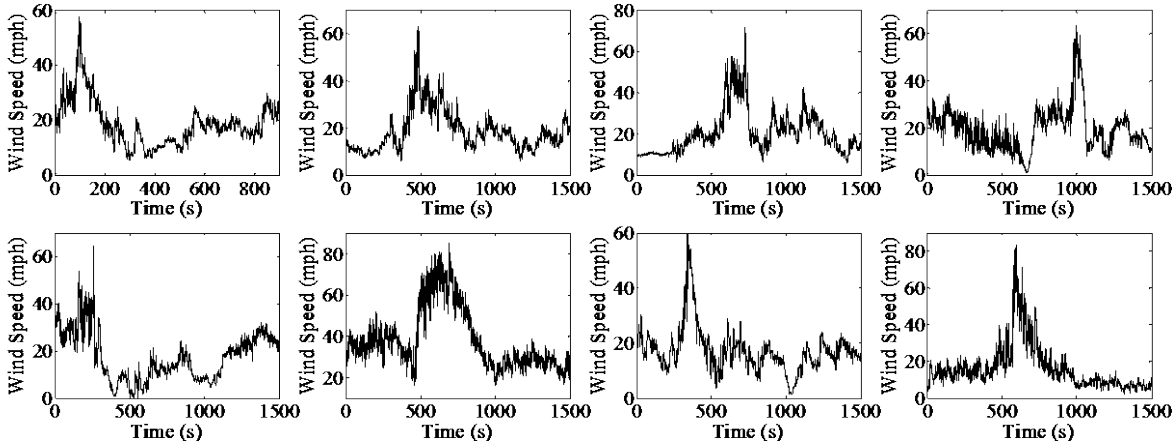

Figure 3: A family of downburst type events recorded (Lombardo, 2010).

The data in figure 3 follows on from the high quality and ongoing work at Texas Tech University where an array of ultrasonic anemometry has been used to obtain full-scale data relating to transient events. On the 4th June 2002, velocity data relating to the structure of the Texas Rear Flank Downdraft (TRFD) was obtained from 11 anemometers positioned on 7 vertical towers. The towers were evenly spaced at a horizontal distance of 263m apart. Anemometers were located on the central tower at distances heights of 3m, 4m, 6m, 10m and 15m above the ground. Full details of this event can be found in Gast and Schroeder (2003), Chen and Letchford (2005), Chen and Letchford (2006), Orwig and Schroeder (2007) and Holmes et al. (2008).

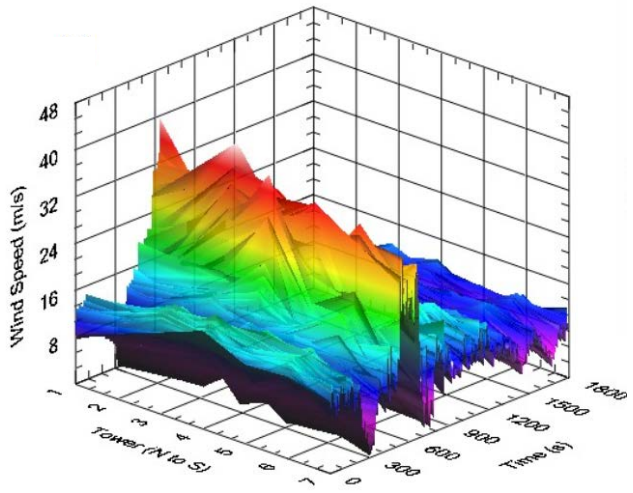

Figure 4: The three dimensional structure of the TRFD (Gast and Schrodeder, 2003).

The number of papers arising from an analysis of the data relating to the TRFD gives an indication of the importance of this event. As illustrated in figure 4, the TRFD provided unique information relating to the spatial and temporal correlation of a singular downburst event.

To illustrate the differences and similarities between the velocity time series for two events, the AAFB and a selection of the TRFD data are shown in figure 5. The TRFD data in figure 5 was obtained at 4m above the ground. It can be observed that both events have similar

characteristics, i.e., relatively low wind speeds prior to the event ($t < -200s$), a significant increase in wind speed when the event is recorded by the anemometers ($t = 0$) and a reduction in wind speed followed by a corresponding secondary peak (which, as shown in figure 3, is not always present in the data). Again, these large changes in wind speeds over a relatively short period of time are different from what is typically observed in synoptic winds.

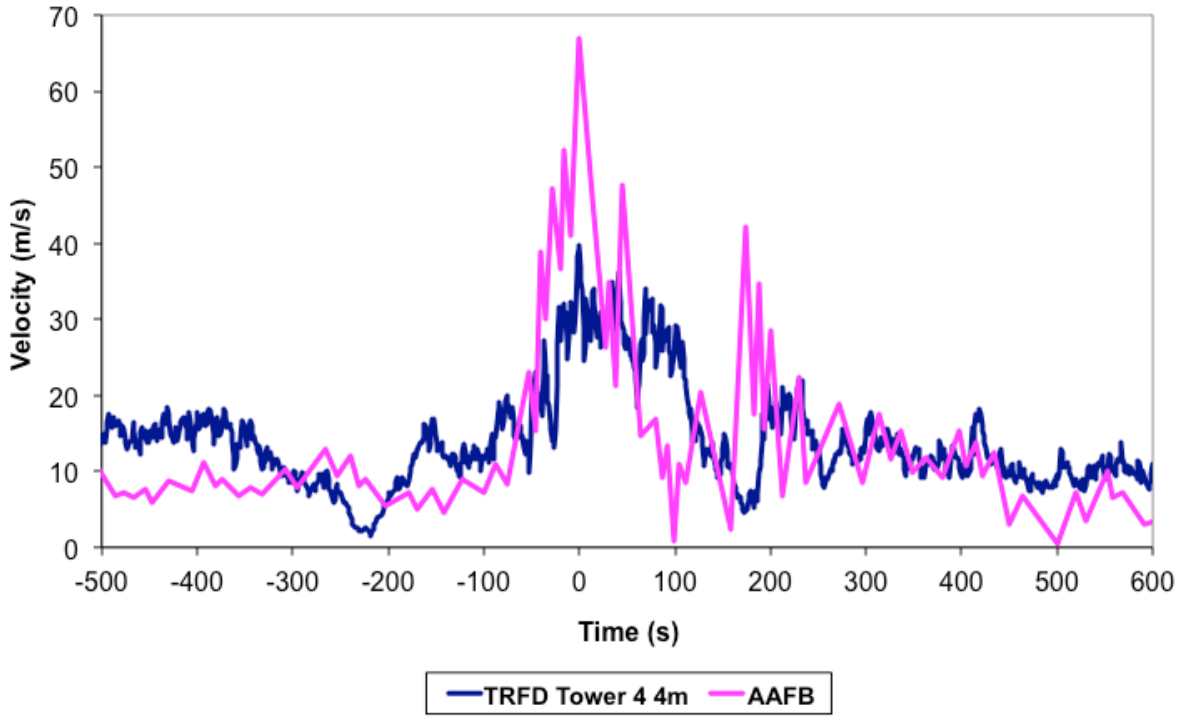

Figure 5: Field data relating to the AAFB event and TRFD from tower 4 (4m above the ground). The TRFD data has been interpolated and hence smoothed to enable a direct comparison with the AAFB data.

The Tuas events are perhaps the most extensive in terms of the number of downburst events recorded. Choi (2004) reports data relating to 50 thunderstorm events and suggests that there are typically of the order of 100 thunderstorm days per year in Tuas (Singapore). The data recorded relates to velocity, temperature and humidity measurements from a 150m tall tower, with sensors located at heights of 35.7m, 62m, 80m and 152m above the ground. This data confirms the general trend in the streamwise velocity with respect to time during an event, i.e., a rapid increase in wind speed corresponding to the passing of the initial gust front. Choi (2004) suggested that events could be classified into four distinct groups depending on the profile shape and the height of the highest wind speed.

Durañona et al. (2007) examined 11 extreme non-synoptic events from velocity data obtained over costal and rural terrain in various locations in Northern Europe. Durañona et al. were careful to note that not all extreme events are associated with downbursts and did not imply that any of the data examined were related to thunderstorm events. Their analysis was concerned with the general velocity distributions and underlying gust structure of an extreme event, which they defined as occurring when "*the local velocity increases rapidly by 50% or more and decreases within a relatively short period of time*". The data analyzed was obtained from www.WindData.com, a database which, at that the time, contained 162,600 hours worth of

meteorological data representing 74 different sites. The study was restricted to data obtained in relatively flat locations where the effect of topographical features such as hills would be negligible. Figure 6 is an example of the data relating to the events occurring at the energy research centre (ECN) in the Netherlands. In figure 6a the vertical axis represents the instantaneous wind speed normalized by the maximum wind speed. In order to visualize the event the velocity data has been filtered using a one minute running average. The vertical lines in figure 6a corresponding to the velocity profiles shown in figure 6b (in which z denotes the height above the ground). The relatively rapid increase in velocity is similar to that observed above (e.g., figure 5), whereas the vertical velocity distribution (figure 6b) illustrates that this is where the similarities end.

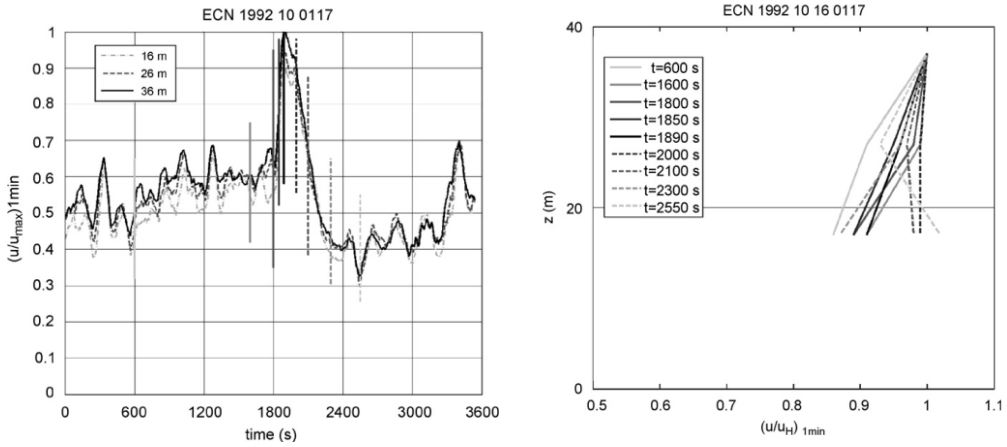

(a) velocity time series (b) velocity distribution

Figure 6: An extreme event at ECN showing (a) the velocity time history and (b) the distribution of velocity with respect to height above the ground. (Durañona et al., 2007).

Durañona et al. (2007) examined the turbulence structure of a number of the events in detail and showed that higher energy was present at smaller scales (compared to synoptic winds) but hypothesized that this was a result of vortex stretching (arising as a result of the rapid increase in local wind velocity) transferring relatively more energy in the smaller length scales. Since such phenomena can also occur in synoptic winds they concluded that "*..despite initial appearances the actual turbulence structure of the flow does not change significantly during the identified wind events and its characteristics would be comparable to those of a normal boundary layer flow."* Similar conclusions were also made by Holmes et al. (2008) who examined the TRFD data. Holmes demonstrated that if the data were filtered appropriately then the "*spectral and correlation characteristics of the residual turbulence [were] found to be similar to those of high frequency turbulence in boundary-layer winds*".

3 PHYSICAL MODELLING OF TRANSIENT WINDS USING THE UNIVERSITY OF BIRMINGHAM SIMULATOR

A number of attempts have been made to physically simulate transient winds, mainly focusing on either thunderstorm downbursts (Chay and Lecthord, 2002; Lin and Savory, 2006; McConville et al., 2009; Mason et al. 2009) or tornadoes (Sengupta et al., 2008). For the sake of brevity, in what follows attention will be restricted to the University of Birmingham's transient wind

simulator.

3.1 A description of the facility

The simulator uses nine axial flow fans, each with a cross sectional area of 0.85m^2 to create a downward jet of air. Immediately below the fans a honeycomb grid of dimensions 10mm by 10mm with a thickness 100mm is positioned to reduce swirl. A transition section downstream of the honeycomb transitions the flow from a square cross section to a circular cross section of diameter (D) (figure 7). Eight triangular flaps are hinged 100m below the end of the circular cross section and are used to generate a downward gust, i.e., prior to the opening of the fans the flow is directed in a horizontal direction and is expelled at a height of 2m above the ground. Once the flaps are released, the weight of the flaps and pressure arising from the jet drive the flaps apart and the flow impinges on the ground and spreads out. As illustrated in figure 8, a ring vortex is created which is driven radially outwards from the point of impingement.

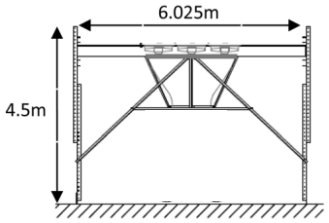

Figure 7: Schematic of the University of Birmingham transient wind simulator.

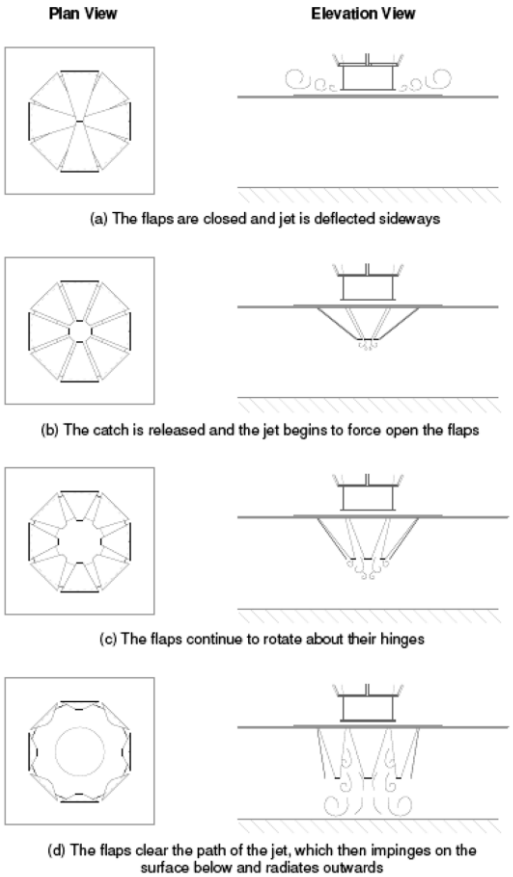

Figure 8: An illustration of depicting plan and elevation views at four stages (a-d) of the opening mechanism (McConville et al., 2009).

As discussed in Sterling et al. (2011) there are a number of issues associated with scaling such physical simulations and the most appropriate scaling may not necessarily be self consistent. The lack of full-data and the variability noted above makes this issue somewhat challenging. Notwithstanding these issues, there is still merit in examining the velocity field and corresponding pressures that arise as a result of such a simulation.

3.2 Velocity flow field

The velocity field was mapped using an array of four Turbulent Flow Instruments (TFI) Cobra probes which measure the 3-D velocity and pressure at a rate of 2kHz. These probes were situated at 10mm intervals along a tangent to the simulated circular gust front, with y = 0mm being on the radius. As discussed previously, the full-scale data show marked differences between different downburst events, though with an underlying consistency in some of the major features. Similarly, velocity time-series from experimental runs show run-to-run variation and, as the aim of this work is to characterize a "typical" downburst event, a multi-run mean time-series was calculated at each point, as used by McConville (2008). At each position, ten experimental runs were conducted. In order to eradicate indexing differences due to inconsistency when starting the data recording, the data from each were synchronized by the first exceedence of a limiting value, and the run-mean value of each instantaneous velocity calculated. This run-mean series was smoothed using a 50-point moving average. While the process of mapping the velocity field fully is ongoing, the mapping of four vertical sections around y = 0mm, at a radial distance of x/D = 2.0, has been completed and the results are presented here.

Taking into account the background wind fluctuations seen in the full-scale time-series of figure 3, the experimental run-mean time series (of which a typical example is shown in figure 9) show a qualitative match with a number of the full-scale time-series. Due to the scaling issues discussed earlier, a quantitative analysis will not be meaningful until the velocity field has been mapped at other radial distances. This qualitative match is promising for the ability of the future work to provide useful data.

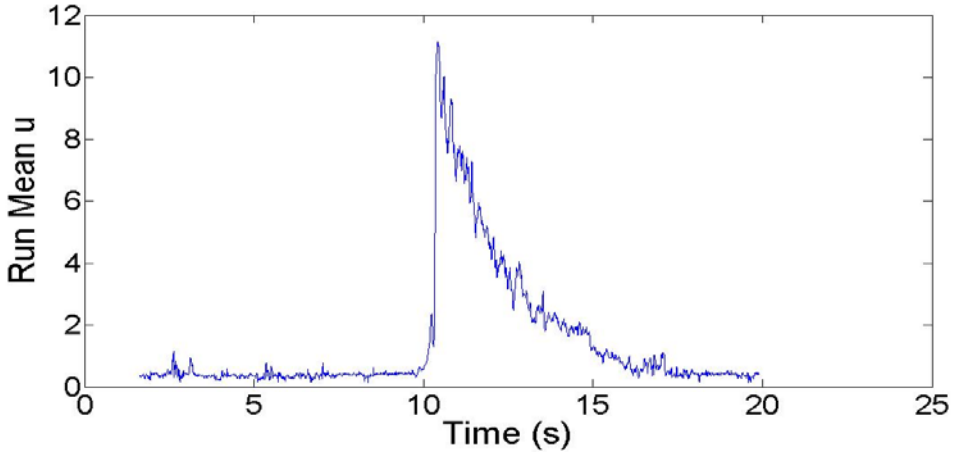

Figure 9: Radial velocity run-mean time-series at x/D = 2.0, y = 0mm, z = 30mm.

Of interest in figure 9 is the velocity dip seen just after t = 10s. This is evident in all time-series at z < 50mm but is not seen in those time-series above approximately 90mm (figure 10). From flow visualization it is estimated that the primary, ring vortex is approximately 0.5m high. In numerical simulations, Mason (2009) saw a secondary vortex forming at the leading edge of the

primary vortex, of diameter approximately half the height of the primary vortex. Further analysis is needed, but it is tentatively speculated that this velocity dip may be evidence of such a vortex forming in the transient wind simulator.

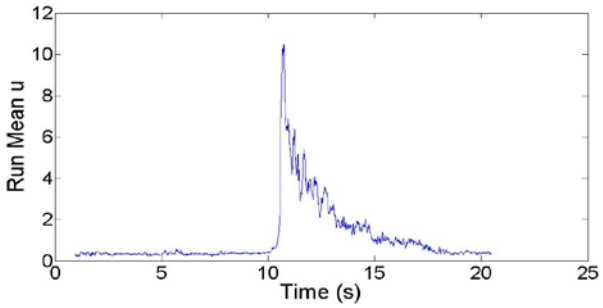

Figure 10: Radial velocity run-mean time-series at x/D = 2.0, y = 0mm, z = 130mm.

If the simulations are to provide useful data, it is of great importance that the velocity field generated is spatially representative of a downburst event, as well as temporally. The vertical velocity profile must therefore be compared to that seen for downburst winds (figure 11). It may be seen that in the region of the flow where the radial velocity, u, has its highest values, u is approximately constant over a range of heights. Due to this there is the potential for small variations in u to disproportionately shift z_{max}, the height at which the maximum velocity, u_{max} occurs. In order to meaningfully non-dimensionalise the data it was necessary to estimate z_{max} as z_{max} = 60mm, the centre of the constant u region. It is evident from comparison with figure 2a that the vertical velocity distribution is unlike that for ABL flow, while the work of Hjelmfelt (1988) provides a basis for comparison with full-scale downburst data. Hjelmfelt examined the vertical velocity profiles of eight downbursts detected as part of the JAWS project and its offspring projects, and calculated a mean profile from these. All four vertical sections measured in the simulator approximate Hjelmfelt's profile, with a near-ground maximum velocity and a sharp decrease as z→0.

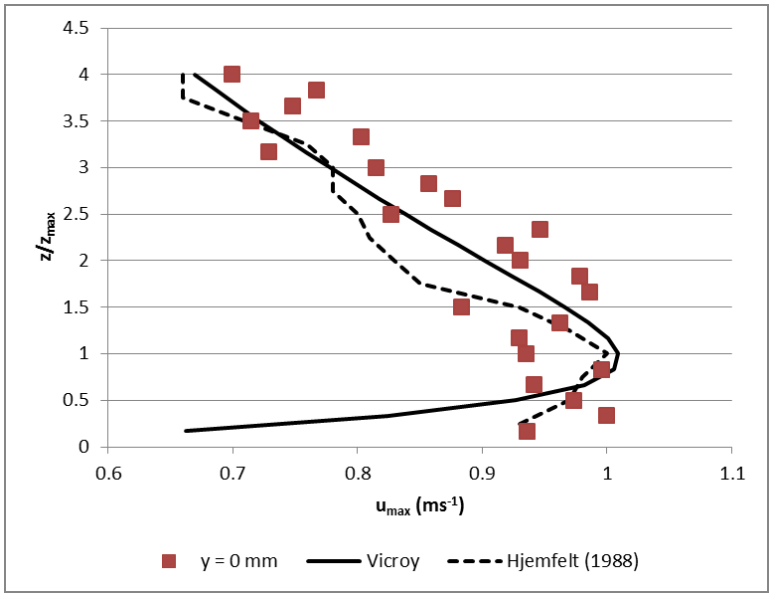

Figure 11: Vertical velocity profiles from the simulator, full-scale data and vertical velocity profile.

3.3 Wind induced pressures

In order to gain an insight into the pressures that may occur on a '*high-rise*' building as a result of a potential downburst, a 244mm x 98mm x 104mm was placed in the flow with a series of pressure tappings on the centre line of the building (figure 12).

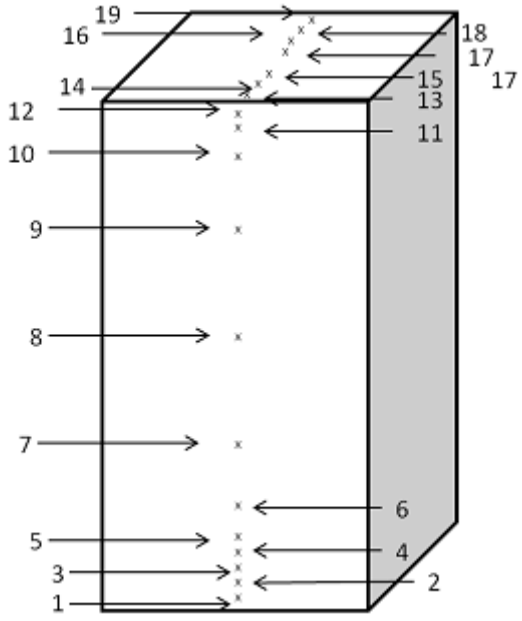

Figure 12: The arrangement of pressure taps on the model building.

The location of the pressure taps is defined in terms of distance from the ground on the windward face measured around a line extending over the central portion of the building. For example, a tap on the windward face at the base would have a position of 0mm while a tap on the base of the leeward face would have a position of 592mm. In what follows the location of the taps have been expressed in terms of a normalised distance, i.e., the distance from the base of the building at the leading edge divided by 592mm. Hence, the location of the taps, illustrated in figure 12 are: tapping 2 (0.0338), 4 (0.0676), 8 (0.2061), 10 (0.3784), 12 (0.4037), 13 (0.4206), 15 (0.4747), 16 (0.5000), 17 (0.5253), 19 (0.5794), 22 (0.6149) and 24 (0.7872). The current results relate to a building positioned at a distance (X) of 1m from centre of the impingement (i.e., X/D = 1.0). The pressure data are expressed in coefficient form:

$$C_{pE}(t) = \frac{P(t) - P_{ATMOS}}{\frac{1}{2}\rho U^2} \tag{1}$$

where P(t) represents the instantaneous pressure, P_{ATMOS} is the atmospheric pressure, ρ is the density of air and U is the smoothed streamwise velocity data corresponding to a full-scale height of 10m. At this stage it is worth expressing a note of caution. Due to the uncertainties

associated with scaling such a simulation, the location of the equivalent full-scale height can be open to interpretation. Hence, since the velocity distribution varies with respect to height above the ground a large degree of uncertainty in the denominator can be expected. The practical implications of this are that the pressure coefficient data should not be considered as absolute.

Figure 13 illustrates the pressure distribution (expressed in coefficient form) around the building. In figure 13, the solid thick black lines represent the building and the ground, the dotted black lines represent a zero datum, while the rectangular black symbols connected by thin black lines provide an indication of the pressure distribution. When the latter is towards the building this indicates a negative pressure, while away from the building indicates a positive pressure. The three blue lines provide an indication of average pressure distribution corresponding to a boundary layer wind. Finally, the upper left and right figures provide an indication of the streamwise and vertical velocity (w) time histories respectively – the vertical red line in both figures illustrates the time to which the pressure data corresponds. The velocity data is provided for illustration purposes only.

Figure 13 illustrates some interesting behaviour. As would be expected there is a large positive pressure on the windward face of the building which for the majority of time exceeds the scale adopted. However, it is noteworthy that pressure closer to the bottom of structure is larger than that further away from the ground, i.e., opposite to what one would expect in boundary layer flow. The pressure on the roof rarely exceeds its boundary layer equivalent and alternates between positive and negative, which is probably as a direct result of the w component. The most interesting feature of the pressure distribution can be observed on the leeward face which shows relatively large positive pressures for most of the time. This is in sharp constant to similar observations concerning boundary layer wind induced pressures where one would expected a large degree of negative pressure to exist in the lee of the building. In order to explore this issue further a series of limited flow visualization experiments were undertaken (figure 14).

In figure 14 to the flow is from left to right and non-neutrally buoyant particles have been used to provide a qualitative indication of the flow behavior. Figure 14a illustrates the flow as the ring vortex is just upstream of the building whereas figure 14b provides an insight into the flow field as the ring vortex passes the building. It is evident from figure 14b that a number of particles have been lifted into the flow and pressed against the windward face of the building. This supports the positive pressure behavior highlighted in figure 13. This point will be examined further in section 4.

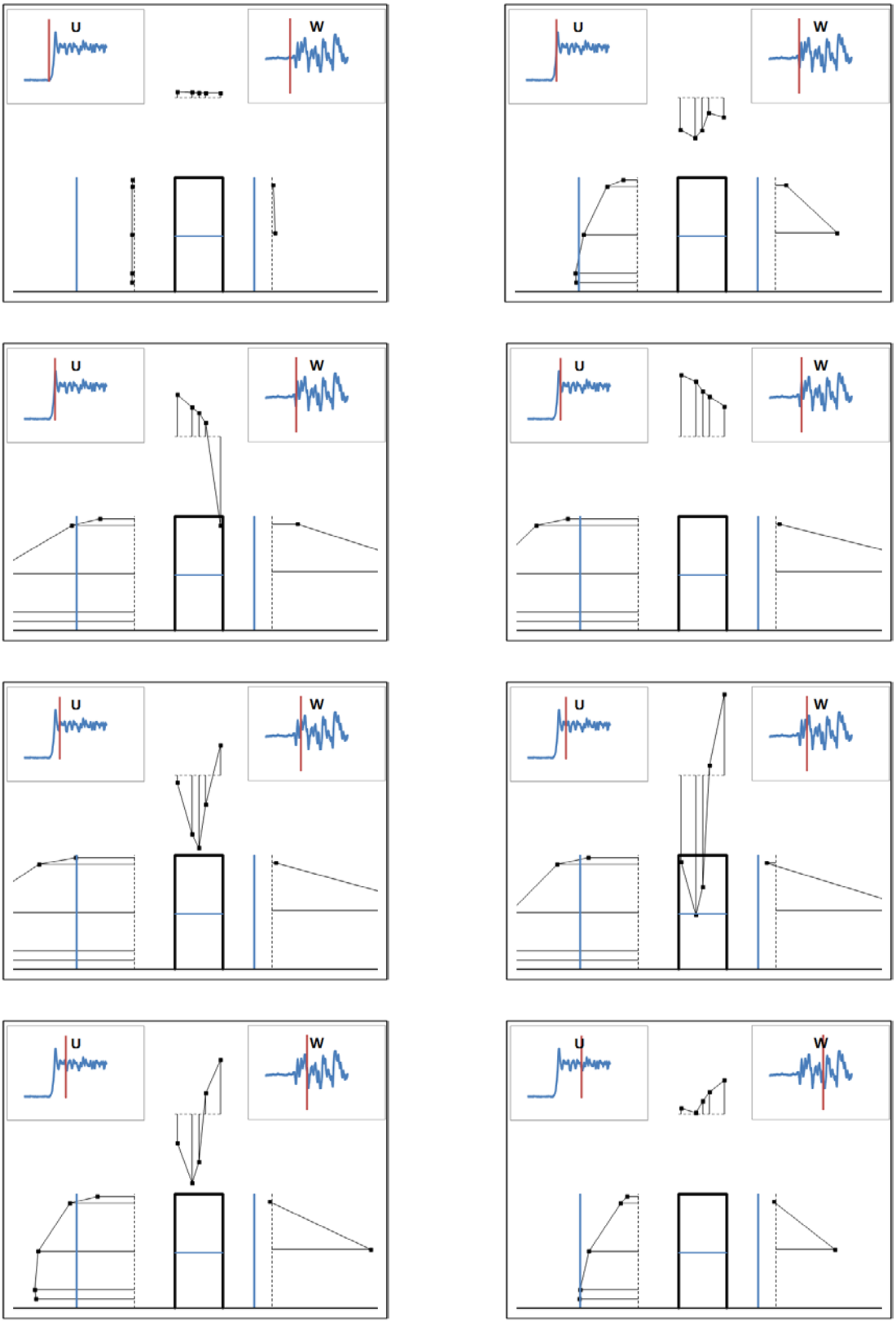

Figure 13: Instantaneous pressure distributions around a physical model of a ‘high-rise’ structure.

(a) before the impact of the ring vortex (b) after the impact of the ring vortex

Figure 14: Flow visualization around a model building.

4 NUMERICAL SIMULATIONS

With the recent increase in computational power, numerical simulations are being more frequently used to simulate thunderstorm downbursts in a variety of ways. Research is tending to fall broadly into two disciplines; simulating the physical mechanisms of a downburst, either using some form of meteorological model or simulating the physical simulators being used for research.

Previous meteorological models have included, but are not limited to, Procter (1988), Orf et al. (1996) and Mason et al. (2008). Procter (1988) and Procter (1989) used a numerical model (the Terminal Area Simulation System, axisymmetric version) to examine precipitation driven downbursts and obtained vertical velocity profiles closely matching doppler radar campaigns of the time. Both Orf et al. (1996) and Mason et al. (2008) modelled a downburst by introducing a cool plume of air into the upper atmosphere which then sank due to buoyancy effects; these models did not include the affects of moisture cloud microphysics but produced results which matched reasonably with actual downburst events. The most recent model has been developed by Lin et al. (2007) which uses the CM1 cloud microphysics model (Bryan & Fritsch, 2002), a moist non-hydrostatic model, to simulate a downburst event. While the model itself produced profiles very similar to profiles captured by Doppler radar and other measurement campaigns there are difficulties in using such a model. Extracting the wind fields to allow calculations of pressures around buildings and hence wind loads is difficult due to the complexity of the model and difficulty in predicting where the downburst will fall. This would make the potential placing of terrain used to simulate model buildings difficult. They are also very computationally expensive to run.

The other method is to simulate the various types of impinging jet simulator, with numerical models using either URANS or LES having been used for this purpose. There are some advantages and disadvantages to this approach. One of the main advantages is that it is relatively simple to calibrate the model as data from the simulator can be used to provide initial conditions and to check the simulation is progressing as expected. However, the physical mechanism used in the impinging jet simulators differs greatly from that of a real downburst event. Previous work by Letchford et al. (2002), Mason et al. (2005), Lin & Savory (2006) and McConville et al. (2009) has shown that velocity time histories can match reasonably well. However, Sterling et al. (2011) discusses the problem of scaling such simulations. The question then arises as to how to

calculate the pressure coefficients around a building given the scaling problems discussed. These problems are inherent to impinging jet type simulators and are not likely to disappear in the near future, nor is an alternative solution likely to present itself, and so such problems should (for now) always be considered when analysing data.

One of the first such numerical impinging jet simulations was by Selvam & Holmes (1992) who carried out a 2-d steady state impinging jet simulation to examine if a simplified model could come close to the work of Procter (1988). The model on the whole captured the vertical velocity profile successfully with a slight overestimation towards lower altitudes due to known problems with the k–ε model overestimating turbulence in regions of high shear. Recent work by Zhou et al. (2011) used LES simulations of an impinging jet to look at a wind field on a solar updraft tower and the possible wind loading implications this might have. They found that the simulated wind loading produced a pressure field similar to that seen by Fujita & Wakimoto (1981) in early studies of thunderstorm downbursts and would have the potential to load the tower in a different manner to synoptic winds.

4.1 Description of approach adopted

The use of CFD at the University of Birmingham was used initially to help visualize what was happening around the model building in section 3. A simulation was set up using OpenFoam with the numerical domain was considered as a 10m x10m x 2.5m box with an .stl file used to simulate the inlet and also used to simulate a high rise building. The mesh and general set up can be seen in figure 15.

The roof and floor of the simulation are modelled as walls with the sides acting as outlets. The inlet condition was initially modelled as a jet with a turbulence intensity of 2% and a of velocity 13.7 m/s. Later simulations adjusted this to 13% to more closely match the flow from the jet in the simulator. The inlet condition was also time-varying with the jet being initially "on" before being turned off after 1s. The outlets were set up as follows: if flow goes in the direction out of the domain ($\varphi < 0$) then a Neumann (zero gradient) boundary was assumed. If the flow attempted to reenter the domain ($\varphi > 0$) a Dirichlet boundary condition of zero velocity was supplied. φ is the flow rate through the boundary face given as the dot product of the velocity vector with the vector normal to the boundary face.

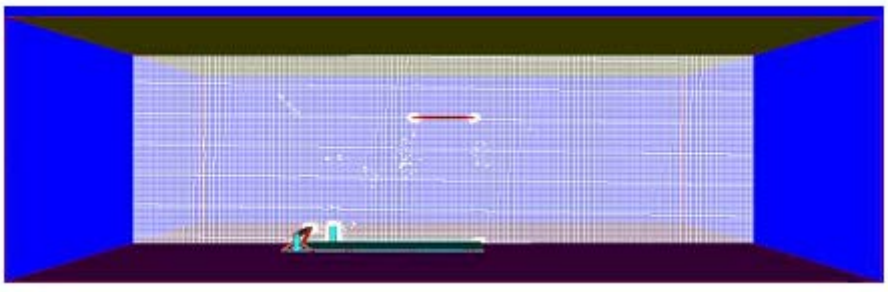

Figure 15- Overview of preliminary numerical simulation domain.

4.2 Velocity flow field

The simulation itself was run for 2s, which gave time for the flow to cease after the jet was

turned off. As with the physical simulator, pulsing the jet in this manner enabled an examination of the vortex structures which formed in the model rather than looking solely at the steady state impinging jet that would otherwise develop.

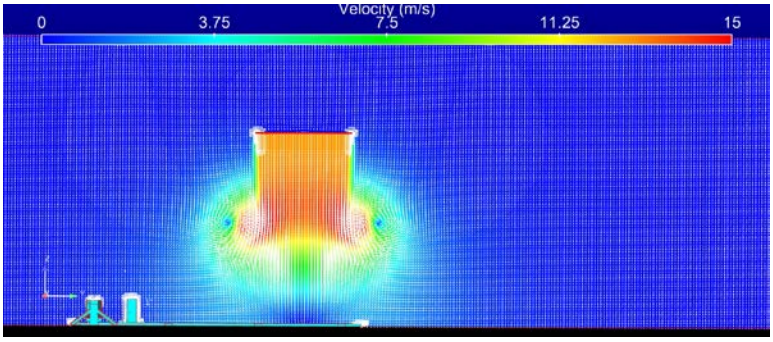

a: Time 0.2s

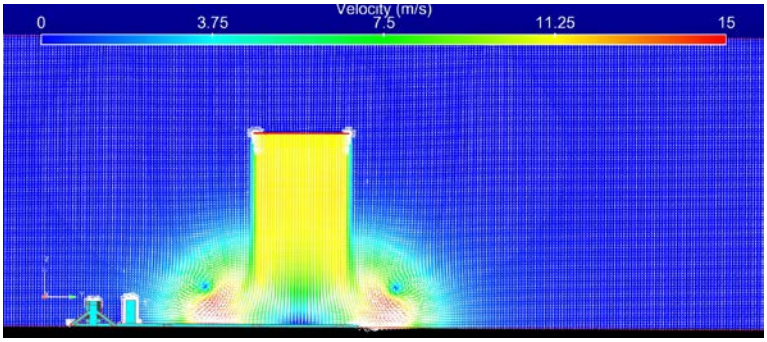

b: Time 0.35s

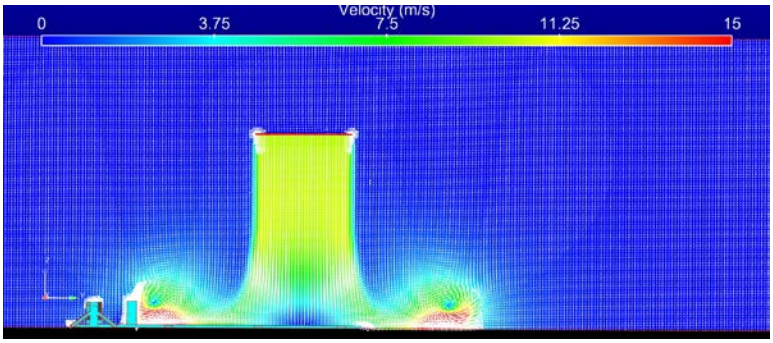

c: Time 0.45s

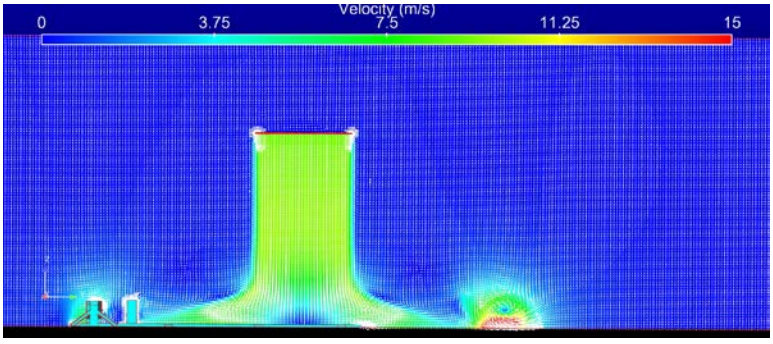

d: Time 0.55s

Figure 16: Overview of preliminary numerical simulation domain.

The vortex initially begins to develop from the shear layer between still air and the jet as is illustrated in figure 16a, and then spreads along the floor (figures 16b – 16d). The flow around the building is illustrated in more detail in figure 17. As with the flow visualisation experiments seen in section 3, a flow reversal can be seen on the building (figure 17b).

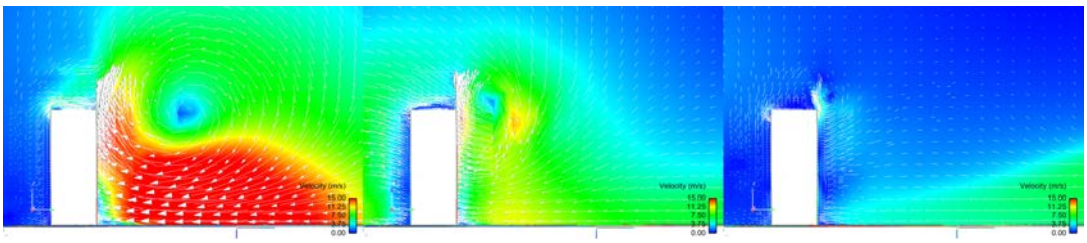

(a) Time 0.45s (b) Time 0.5s (c) Time 0.55s

Figure 17. Flow around the building

5 CLOSING REMARKS

This paper has examined a number of issues associated with transient winds and in particular thunderstorm downbursts. Care has been taken to stress the uniqueness of each downburst event and to highlight the similarities and differences that are likely to be present in the velocity flow field. A series of flow visualization events, pressure field measurements and numerical simulations have been presented in order to examine the flow field associated with a possible downburst as it impacts on a high-rise building. The main difference when compared to stationary wind events appears to be the large positive pressure that can occur on the leeward side of the building. However, given the scaling issues associated with such simulations these results should be interpreted with care.

REFERENCES

Bryan, G.H., & Fritsch, J.M. 2002. A Benchmark Solution for Moist Nonhydrostatic Numerical Models. Mon. Wea. Rev., 130, 2917–2928.

Chen, L. and C. Letchford, 2005: Proper orthogonal decomposition of two vertical profiles of full-scale nonstationary downburst wind speeds. *Journal of Wind Engineering and Industrial Aerodynamics*, 93(9), 187–216.

Chen, L. and C. Letchford, 2006: Multi-scale correlation analyses of two lateral profiles of full-scale downburst wind speeds. *Journal of Wind Engineering and Industrial Aerodynamics*, 94(9), 675–696.

Chay, M.T., & Letchford, C.W. (2002). Pressure distributions on a cube in a simulated thunderstorm downburst, Part A: stationary downburst observations. Journal of wind engineering and industrial Aerodynamics, 90, 711–732.

Choi, E., 2004: Field measurement and experimental study of wind speed profile during thunderstorms. *Journal of wind engineering and industrial Aerodynamics*, 92, 275–290.

Durañona, V., Sterling, M and Baker, C. J (2009) An analysis of extreme non-synoptic winds. *Journal of Wind Engineering and Industrial Aerodynamics*. 95, 1007-1027.

Fujita, T., 1985: Downburst: Microburst and macroburst. University of Chicago Press, IL, pp. 122.

Fujita, T.T., & Wakimoto, R.M. 1981. Five scales of airflow associated with a series of downbursts on 16 July 1980. Monthly weather review, 109, 1439–1456.

Gast, K. and J. Schroeder, 2003: Supercell rear-flank downdraft as sampled in the 2002 thunderstorm outflow experiment. *11th International conference on Wind Engineering,* Lubbock, Texas, ICWEIA, Vol. 2, 2233–2240.

Haines, M., Sterling, M and Quinn A. D (2012) The simulation of non-synoptic effects for wind damage studies. *The seventh international colloquium on bluff body aerodynamics and applications (BBAA7).* Shanghai, China, September 2-6, 2012.

Hjelmfelt, M. R (1988) Structure and life cycle of microburst outflows observed in Colorado, Journal of Applied Meteorology 27 (1988) 900-927.

Holmes, J., H. Hangan, J. Schroeder, C. Letchford, and K. Orwig, 2008: A forensic study of the lubbock-reese downdraft of 2002. *Wind and Structures*, 11(2), 137–152.

Kareem, A (2012). Modelling of transient Wind and their load effects on structures. *10th UK Conference on Wind Engineering,* Southampton, 10-12th September 2012.

Lin, W. and Savory, E (2010) Physical modelling of a downdraft outflow with a slot jet. *Wind and Structures*, 13, 385–412.

Lin, W.E., & Savory, E. (2006) Large-scale quasi steady modelling of a downburst outflow using a slot jet. Wind and structures, 9, 419–440.

Lin,W.E., Orf, L.G., Savory, E., & Novacco, C. (2007). Proposed large-scale modelling of the transient features of a downburst outflow. Wind and structures, 10, 315–346.

Letchford, C., C. Mans, and M. Chay, (2002): Thunderstorms - their importance in wind engineering, a case for the next generation wind tunnel. *Journal of Wind Engineering and Industrial Aerodynamics*, 90, 1415–1433.

Lombardo, F T (2010) Analysis and interpretation of thunderstorm wind flow and its effects on a bluff body. PhD thesis. Texas Tech University.

Mason, M., Letchford, C. W and James, D (2005) Pulsed wall jet simulation of a stationary thunderstorm downburst, part a: Physical structure and flow field characterization. *Journal of Wind Engineering and Industrial Aerodynamics*, 557–580.

Mason, M.S., Wood, G.S., & Fletcher, D.F. (2008). Numerical simulation of downburst winds. Journal of Wind Engineering and Industrial Aerodynamics, 97, 523–529.

McConville, A., 2008: The physical simulation of thunderstorm downbursts. PhD thesis, University of Birmingham, 236 pp.,

McConville, A., A. Sterling, and C. Baker, 2009: The physical simulation of thunderstorm downdrafts using an impinging jet. *Wind and Structures,* 12(2), 133–149.

Orf, L.G., Anderson, J.R., & Straka, J.M. 1996. A three-dimensional numerical analysis of colliding microburst outflow dynamics. J. Atmos. Sci., 53(17), 2490–2511.

Orwig, K. and J. Schroeder, 2007: Near-surface wind characteristics of extreme thunderstorm outflows. *Journal of Wind Engineering and Industrial Aerodynamics*, 95, 565–584.

Procter, F.H. 1988. Numerical simulations of an isolated microburst. Part I: dynamics and structure J. Atmos. Sci., 45(21), 3137–3160.

Procter, F.H. 1989. Numerical simulations of an isolated microburst. Part II: sensitivity experiments J. Atmos. Sci., 46(14), 2143–2165.

Sengupta, A., Hann, F. L., Sarkar, P and Balaramudu, V (2008) Transient loads on buildings in microbursts and tornado winds. *Journal of Wind Engineering and Industrial Aerodynamics*, 96, 2183-2187.

Selvam, R.P., & Holmes, J.D. 1992. Numerical simulation of thunderstorm downdrafts. Journal of wind engineering and industrial aerodynamics, 44(4), 2817–2825.

Sterling, M, Baker, C. J., Haines and Quinn A. D. (2011) Scaling a thunderstorm downburst simulator. *13th International Conference on Wind Engineering*. 11th – 15th July,

Amsterdam, the Netherlands.
Zhou, Xinping, Wang, Fang, & Liu, Chi. 2011. Wind pressure on a solar updraft tower in a simulated stationary thunderstorm downburst. Wind and structures, 15(4), 331–343.